



Drought and UV-B radiation modulate *Adenanthera pavonina* leaf metabolite profile and physiology

Maria Celeste Dias^{1,2} · Diana C. G. A. Pinto² · Maria Costa² · Conceição Santos³ · Artur M. S. Silva²

Received: 9 September 2022 / Revised: 21 December 2022 / Accepted: 21 October 2023 / Published online: 13 November 2023
© The Author(s) 2023

Abstract

Adenanthera pavonina is a medicinal species, which economic value depends on the richness of its phytochemicals. Extreme climatic conditions are becoming frequent worldwide, but despite their impact on plant productivity these weather events also modulate plants' metabolism increasing the production of important phytochemicals. We aimed to characterize the physiological and metabolite adjustments in *A. pavonina* leaves induced by drought and UV-B radiation. Plants were exposed to drought (DS), UV-B radiation (UV-B), and drought + UV-B (DS + UV-B), and photosynthesis, lipophilic metabolites, and antioxidant status were evaluated. The stress conditions compromised the photosynthetic performance and induced oxidative stress (DS and UV-B plants). However, plants activated protective mechanisms (increased antioxidant activity and flavonoids in all treatments, total phenols in DS and DS + UV-B, and catechols in UV-B and DS + UV-B) and modulated their lipophilic profiles (accumulation of fatty acids and TCA cycle-related metabolites, and reduction of carbohydrates) to cope with the stress. We demonstrate for the first time that DS and UV-B radiation can enrich *A. pavonina* leaves with antioxidants and fatty acids increasing their medicinal value.

Keywords Climate conditions · Medicinal plants · Metabolite profile · Antioxidants · Photosynthesis

Introduction

Due to climate change, the frequency of extreme weather events is forecasted to increase in the next decades (IPCC 2014), influencing forest- and agro-ecosystems. Drought is one of the most persistent stressors, and to adapt to drought, plants change root growth and architecture and alter their physiology (e.g., hormone signalling cascades and stomata closure). These modulations modify the flux of cellular

signals, that can result in a decline of growth and yield (Ma et al. 2020). Drought is increasingly being accompanied by UV-B radiation (280–315 nm), which elicits a variety of plant photomorphogenic responses but at high levels may potentially damage plants' DNA, proteins, or other cellular components (Escobar-Bravo et al. 2021).

Under stress conditions, the production of reactive oxygen species (ROS) can increase (Ma et al. 2020). However, plants possess enzymatic and non-enzymatic defence mechanisms that work together to control the levels of ROS and oxidative stress. Secondary metabolites, like flavonoids and hydroxycinnamic acids (Huang et al. 2019), are able to scavenge $O_2^{\bullet-}$, OH^{\bullet} and 1O_2 , especially the *ortho*-dihydroxy B-ring substituted flavonoids that have a high antioxidant capacity (Brunetti et al. 2013). Besides helping plants cope with stressful conditions, the accumulation of these metabolites derives from shifts in the cell secondary metabolism, altering plants' antioxidant and nutritional characteristics (Dias et al. 2020a, 2020b).

Climatic conditions influence important primary and secondary metabolic pathways, changing metabolite profiles that affect several species' pharmaceutical properties (Machado et al. 2017; Gupta et al. 2019). Medicinal plants

Communicated by C.L. Cespedes.

✉ Maria Celeste Dias
celeste.dias@uc.pt

¹ Centre for Functional Ecology - Science for People & the Planet, Associate Laboratory TERRA, Department of Life Sciences, University of Coimbra, Calçada Martim de Freitas, 3000-456 Coimbra, Portugal

² LAQV/REQUIMTE, Department of Chemistry, University of Aveiro, Campus Universitário de Santiago, 3810-193 Aveiro, Portugal

³ IB2, Department of Biology & LAQV/REQUIMTE, Faculty of Sciences, University of Porto, Rua Do Campo Alegre, 4169-007 Porto, Portugal

are rich in specific phytochemicals, being used in popular medicine or raw material for many pharmaceutical and food industries (Omidi et al. 2018). Medicinal species produce a wide variety of free radical scavenging molecules (e.g., phenolics, terpenes/terpenoids, alkaloids, vitamins, and other secondary metabolites), as well as primary metabolites with antioxidant properties (e.g., amino acids, sugars, fatty acids, and intermediates of the tricarboxylic acid (TCA) cycle) (Gupta et al. 2019). UV-B radiation modulates the plant's secondary metabolism leading to the increase of phenolic compounds, namely flavonoids and glucosinolates, depending on the species and dose (Schreiner et al. 2016; Wu et al. 2021).

Adenanthera pavonina L., known as a red lucky seed or red sandalwood tree, is an agroforest species widely cultivated in the tropics (Acevedo-Rodríguez and Strong 2012) in regions currently under high environmental pressure due to climate change. It is a multipurpose species, used as a windbreak, ornamental species, source of wood and animal fodder, and for nitrogen soil fixation (Zarnowski et al. 2004; PROSEA 2012). Its leaves and seeds are highly rich in bioactive compounds (such as flavonoids, alkaloids, coumarins, anthraquinones, saponins, tannins, steroids, triterpenoids, glycosides, carbohydrates and fatty acids), being widely used in traditional medicine and phytotherapy for anti-inflammatory, antidiarrheal, antinociceptive, antimicrobial and anticancer purposes (Geronço et al. 2020). Being an emerging species for the agro-pharmaceutical industry, it is important to know its tolerance to climate change related stressors, such as drought or high UV-B radiation and how these stressors modulate leaf metabolite profile.

The increasing demand of high quality phytochemicals for pharmaceutical and food industries (Omidi et al. 2018) highlights the necessity to address how climate conditions modulate medicinal species performance, including redox status. This study investigates how *A. pavonina* reconfigure its physiology and antioxidant status to cope with drought and high UV-B radiation episodes and unravelling if these stressors improve leaves phytochemicals, promoting their nutritional level and the economic value of this species.

Material and methods

Plant material and treatments

Adenanthera pavonina L. seeds were collected in a Dili orchard (East-Timor). At the University of Aveiro (20/01/2015), seeds were disinfected with commercial bleach at 10%, immersed in sulfuric acid for 20 min, washed 3× with distilled sterile water, and then placed in a petri dish in wet cotton and incubated at 22 ± 2 °C. After 6 to 7 days, seedlings were transferred to plastic pots (300 mL) with a

mixture of turf and perlite (3:1). After 40 days of growing in a climatic chamber at 22 ± 2 °C, a photoperiod of 16 h day, and with a light intensity of $500 \pm 20 \mu\text{mol m}^{-2} \text{s}^{-1}$, plants (Fig. 1) were divided into 4 groups of 8 plants each: control (C, $n=8$), drought stress (DS, $n=8$), ultraviolet B radiation (UV-B, $n=8$) and drought stress + UV-B (DS + UV-B, $n=8$). Before applying the specific treatments, plants were kept watered at 100% field capacity. Control plants were maintained in the same growing conditions and watered during the whole experiment. DS plants remained in the same growing conditions but were not watered for 7 days. Plants from the UV-B treatment were exposed to a total effective dose of 10.8 kJ m^{-2} [5.4 kJ m^{-2} per day, and for 2 days, calculated according to Correia et al. (2012)]. DS + UV-B plants were not watered for 7 days, and at the 6th and 7th days of water holding, plants were exposed to UV-B radiation of $5.4 \text{ kJ m}^{-2} \text{ d}$. A system composed of ten UV-B lamps (Sankyo Denki G8T5E, Kanagawa, Japan), with an energy spectrum of 280–320 nm and an emission peak at 306–312 nm, was used. This system contained a borosilicate glass filter to block radiation below 290 nm (UVC, 0 kJ m^{-2}) (Dias et al. 2018). Light UV-B radiation homogeneity was confirmed every day, before treatments, with a 254 and 312 VLX radiometer (Vilber Lourmat, Marnela-Vallée Cedex, France), and the spectral sensitivity and correction factor determined as described in Correia et al. (2012). According to Dias et al. (2018) this UV-B dose can be considered as moderate. At the end of the treatments, gas exchange and chlorophyll fluorescence were measured in situ in the same leaves. Relative water content (RWC) and cell membrane permeability (CMP) were measured in fresh leaves. Additionally, leaf samples were harvested, immediately frozen in liquid nitrogen, and kept at -80 °C.

Determination of leaf water status, photosynthesis and pigments

Leaves were weighted to determine the fresh weight, and then immersed in water for 24 h at 4 °C to determine the turgid weight. After that, leaves were dried at 80 °C for 3 days to determine the dry weight (Brito et al. 2021). The relative water content (RWC in %) was calculated as $100 \times (\text{leaf fresh weight} - \text{leaf dry weight}) / (\text{leaf turgid weight} - \text{leaf dry weight})$.



Fig. 1 *Adenanthera pavonina* plants after 40 days of growing

Leaf gas exchange, and chlorophyll *a* fluorescence were determined in situ with a portable photosynthesis system LI-6400XT (LI-COR, Lincoln, Nebraska, USA) between 10 and 12 am. Leaf gas-exchange (net CO₂ assimilation rate, transpiration rate and stomatal conductance) measurements were performed at growth ambient conditions and with a light intensity of $500 \pm 20 \mu\text{mol m}^{-2} \text{s}^{-1}$. The intercellular CO₂ concentration and extracellular CO₂ concentration were calculated. For chlorophyll *a* fluorescence, the maximum quantum efficiency of PSII ($F_v/F_m = (F_m - F_0)/F_m$) was determined by measuring the fluorescence signal of dark-adapted leaves after a pulse saturating light ($5000 \mu\text{mol photons m}^{-2} \text{s}^{-1}$, for 0.8 s). Then, leaves were adapted to light, the steady-state fluorescence was determined for 2.5 s, and after exposure to a saturating light for 0.8 s, the maximum fluorescence was averaged. Leaves were shaded for 5 s with a far-red light to establish the F_0' . The effective photochemical efficiency of PSII [$\Phi_{\text{PSII}} = (F_m' - F_s)/F_m'$], the efficiency of excitation energy capture by open PSII reaction centres [$F_v'/F_m' = (F_m' - F_0)/F_m'$], photochemical quenching [$qP = (F_m' - F_s)/(F_m' - F_0')$] and non-photochemical quenching [$\text{NPQ} = (F_m - F_m')/F_m'$] were calculated.

To determine pigments, frozen leaves (~50 mg) were macerated with 1 mL of acetone and 50 mM Tris pH 7.8 (80:20, v/v), and then centrifuged at 5000 g for 5 min at 4 °C. The absorbance was read at 470, 537, 647, and 663 nm. The contents of chlorophylls and carotenoids were determined as described by Sims and Gamon (2002).

Total antioxidant activity, total phenols, catechols, and flavonoids

For the total antioxidant activity, total phenols, catechols, and flavonoids, 100 mg frozen leaves were macerated with 1.25 mL of methanol and incubated for 30 min at 40 °C. Then, the homogenate was centrifuged at 5000 g for 15 min at 4 °C, and the supernatant was used for analysis. The total antioxidant activity was determined by the ABTS⁺ free cation radical scavenging activity method (Re et al. 1999). The leaf extract (5 μL) was mixed with 200 μL of the ABTS solution [2,20-azinobis(3-ethylbenzothiazoline-6-sulphonic acid)]. After 10 min at 30 °C the absorbance was measured at 734 nm. The total antioxidant activity was determined using a calibration curve prepared with known concentrations of gallic acid. For total phenols quantification, the leaf extract (5 μL) was mixed with 405 μL of a Folin-Ciocalteu mixture and 75 μL Na₂CO₃ (20%). After incubation at 37 °C for 30 min, the extract was read at 765 nm (López-Orenes et al. 2018). Total phenols content was calculated based on a gallic acid standard curve. Catechols were assessed using the molybdate assay. 40 μL of sodium molybdate solution (5% w/v in 50% methanol) was mixed with 5 μL of the leaf extract (Giertych et al. 1999). After 15 min at 20 °C the

absorbance was read at 370 nm and the content of catechols was calculated using a gallic acid calibration curve. For flavonoid quantification, 5 μL of the extract was homogenized with 37.5 μL of methanol (López-Orenes et al. 2018). Then, 75 μL of NaNO₂ at 5% was added, and mixed and 75 μL AlCl₃ at 10% was also added. After mixed and incubated 6 min in dark, 125 μL NaOH (1 M) was added, and the absorbance read at 510 nm. Flavonoid's amount was determined based on a rutin calibration curve.

Oxidative stress markers

Lipid peroxidation was evaluated by quantifying the malondialdehyde (MDA). Frozen leaves (100 mg) were homogenised with 1.5 mL of 0.1% (w/v) trichloroacetic acid (TCA) and centrifuged at 10,000 g for 10 min at 4 °C. An aliquot of the supernatant was added to 20% TCA (w/v) and ascribed as a negative control. Another aliquot was added to 20% TCA (w/v) and 0.5% thiobarbituric acid (w/v) and ascribed as the positive control. The groups of the positive and negative controls were incubated in a water bath at 95 °C for 30 min, cooled and then centrifuged for 10 min at 10,000 g and 4 °C. The absorbance was measured at 440, 532, and 600 nm, and MDA equivalents calculated (Hodges et al. 1999).

The permeability of the cell membranes (CMP) was calculated by the electrolyte leakage (Araújo et al. 2016). Leaves were placed in closed vials with de-ionised water and left all night on a rotary shaker at 22 °C. The electrical conductivity was assessed (*Lt*). Then, leaves were autoclaved at 120 °C for 20 min and conductivity was determined (*LO*) again. Electrolyte leakage (%) was determined as $Lt/LO \times 100$.

Chromatography analysis

Leaves (1 g) were mixed with 150 mL of *n*-hexane, and the homogenate was stirred for 72 h at room temperature. After this extraction, the *n*-hexane was evaporated using a rotatory evaporator and reused in the next cycle. Each cycle was repeated three times. The leaf extracts were dried and silylated. For the silylation, 200 μL of the leaf extracts (~10 mg mL⁻¹) were added to a mixture of 250 μL of pyridine, 250 μL of *N,O*-bis(trimethylsilyl)trifluoroacetamide, 50 μL of trimethylsilyl chloride. Finally, 200 μL of tetracosane (0.46 mg mL⁻¹), the internal standard, were added and then incubated at 70 °C for 40 min. Samples were injected in a gas-chromatography mass spectrometer (GC-MS, QP2010 Ultra Shimadzu) with a capillary column (DB-5 J&W, 30 m \times 0.25 mm id and a film thickness of 0.25 μm) as described previously by Dias et al. (2020a). The peaks of the chromatogram were identified by comparison with library entries of the mass spectra

database (NIST14 Mass spectral and WILEY RegistryTM of Mass Spectra Data) and/or with retention time and mass spectra of standard compounds. For quantification analysis, calibration curves of reference compounds (palmitic acid, octadecane, octadecanol, cholesterol, maltose, and alanine) representative of the major compounds present in the leaves were performed.

Statistical analysis

Parameters were measured in the eight plants ($n = 8$) used in all treatments, except the gas exchange (in C plants, leaves were damaged during measurements), pigments, flavonoids and catechols where the leaf material was sufficient to measure at least five replicates ($n \geq 5$). Data were analysed by One-Way Analysis of Variance or by the Mann–Whitney U Statistic test when the normality failed using the program SigmaStat for Windows version 3.1 (SigmaPlot, Systat Software, San Jose, CA). The significance level was 0.05. Pearson's correlation (Pearson 1895) was performed to determine the linear relationship presented between the dependent variables analyzed, using the program SigmaStat for Windows, version 3.1. (SigmaPlot, Systat Software, San Jose, CA). Fold change was determined in the Microsoft[®] Excel for windows (version 10).

Results

Plant water status and photosynthesis

DS and DS + UV-B treatments induced a significant reduction of the RWC compared to the control (Fig. 2). Control and UV-B plants showed similar RWC values. The F_v/F_m was similar in control and all stressed groups (Fig. 3A). The Φ_{PSII} decreased in DS and DS + UV-B plants, but in the UV-B plants these values were similar to control (Fig. 3B). All stress treatments decreased the F_v'/F_m' , with DS plants showing the lowest value (Fig. 3C). The net CO_2 assimilation rate were similar in control, DS and DS + UV-B plants, only the UV-B plants showed a net CO_2 assimilation rate significantly lower than control plants (Fig. 4A). The transpiration rate in control plants were higher than in the DS, UV-B, and DS + UV-B plants (Fig. 4B). The stomatal conductance in C plants was higher than in the UV-B and DS + UV-B (Fig. 4C). However, DS, UV-B and DS + UV-B showed similar stomatal conductance. No significant differences were observed in the Ci/Ca between control and stressed groups (Fig. 4D). The Ci/Ca in DS + UV-B plants was lower than in UVB plants (Fig. 4D).

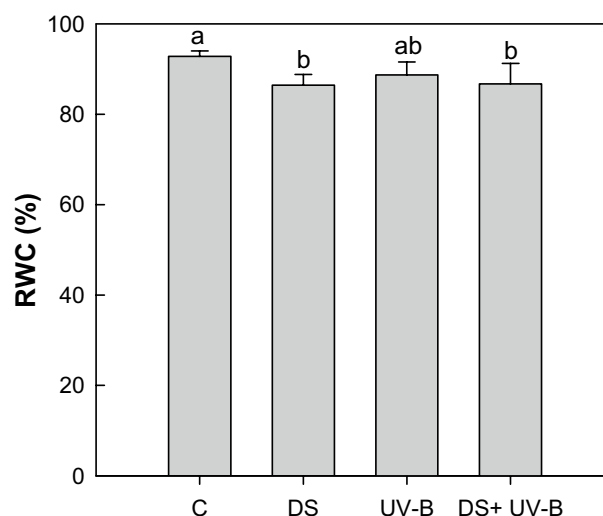


Fig. 2 Leaf relative water content in control, DS, UV-B and DS + UV-B plants of *A. pavonina*. Values are means \pm standard deviation ($n = 8$). Different letters indicate statistical differences between treatments ($p < 0.05$)

Alcohols, carboxylic acids and carbohydrates profiles

Twenty-four compounds were identified, the alcohol triacontanol, the polyols myo-inositol and glycerol, carboxylic acids (stearic, α -linolenic, linoelaidic, palmitic, coumaric, citric, threonic, malic, undecanoic, butanoic, pipercolic and oxalic acids) and carbohydrates [sucrose, turanose, D-trehalose, 3- α -mannobiose, D-glucose (isomer I and II), β -D-galactofuranose, fructose, and D-(-)-tagatofuranose] (Table 1). Triacontanol and glycerol were not detected in DS + UV-B plants. In DS plants, these compounds' levels were significantly lower than the ones of the control and plants exposed to UV-B. Plants exposed to DS and UV-B showed myo-inositol levels lower than control, and this compound was not detected in DS + UV-B plants.

The fatty acids stearic, α -linolenic, linoleic, and palmitic showed a response profile similar in the stressed plants. While control plants had the lowest values, DS plants showed the highest values, followed by UV-B and DS + UV-B plants. The undecanoic and butanoic acids increased in UV-B plants compared with the control, and were undetectable in DS and DS + UV-B plants.

The highest levels of malic acid were found in DS and UV-B plants, while DS + UV-B plants showed the lowest values. Oxalic acid reached maximum and minimum values, respectively, in DS and controls plants, while in DS and DS + UV-B plants its levels were similar. The levels of the organic acids changed according to the conditions. The coumaric, citric, and threonic acids were not found in DS + UV-B

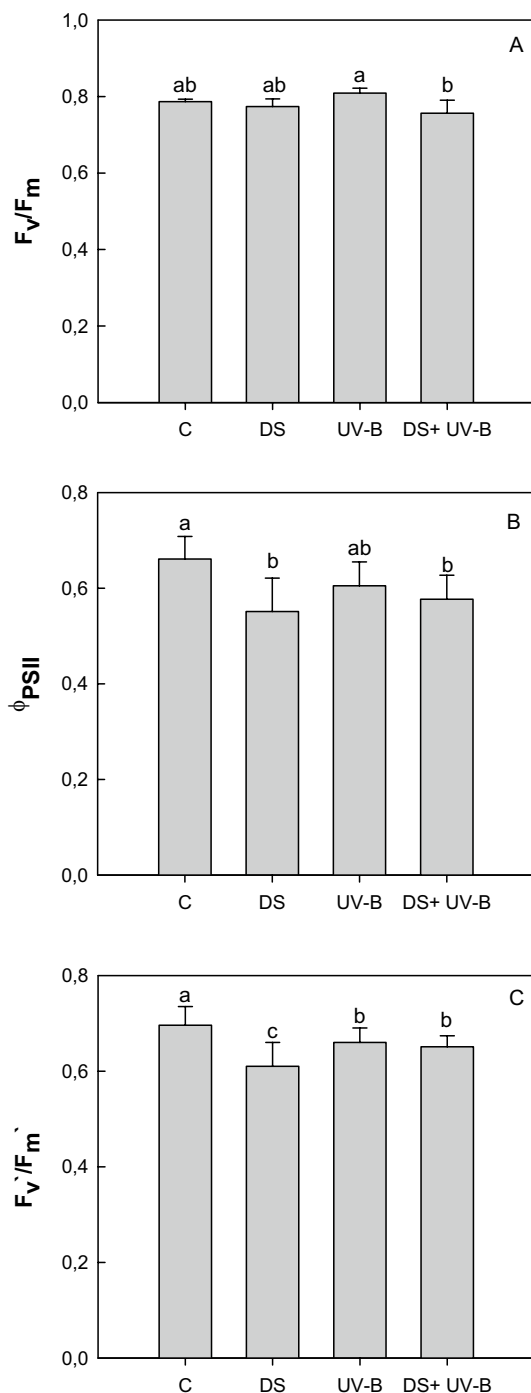


Fig. 3 Maximum efficiency of PSII (F_v/F_m), effective efficiency of PSII (Φ_{PSII}) and efficiency of excitation energy capture by open PSII reaction centres (F_v'/F_m') in control, DS, UV-B and DS+UV-B plants of *A. pavonina*. Values are means \pm standard deviation ($n=8$). Different letters mean statistical differences between treatments ($p < 0.05$)

plants but responded to DS and UV-B treatments. DS showed the highest levels of these three acids, while the control had the

lowest ones. Pipecolic acid reached maximum values in UV-B plants, but was not detected in DS plants.

Regarding carbohydrates, control plants showed the highest levels of D-glucose (isomer I and II), and the DS + UV-B had the lowest values. Control plants also showed the highest sucrose values, which decreased to the lowest detectable levels in UV-B plants and undetectable values in DS + UV-B. Turanose compounds were also higher in control plants, decreasing in stressed plants, with UV-B and DS + UV-B plants showing similar values, and not being detected in DS plants. The sugars β -D-galactofuranose, fructose, and D-(-)-tagatofuranose were not detected in DS + UV-B plants. The contents of D-(-)-tagatofuranose were similar in control, DS and UV-B plants. DS plants showed levels of β -D-galactofuranose significantly higher than UV-B plants, but similar to control plants. Fructose levels were significantly higher in DS, compared to control and UV-B plants. The 3- α -mannobiose was at the highest levels in the control plants and was not detected in DS and DS + UV-B plants. D-trehalose was only identified in control plants.

In Table 1 it is represented the fold changes in metabolites in *A. pavonina* leaves exposed to DS, UV-B, and DS + UV-B conditions. The profile of response of most fatty acids, polyols, and sugars to different stresses is similar, presenting in general a decrease of the respective metabolite, while the profile of carboxylic acids showed a positive response (an increase of these metabolites).

Pigments, oxidative stress and antioxidant response

Plants exposed to DS showed a level of Chl *a* significantly lower than the control plants (Fig. 5A). No changes were observed in Chl *b* content between treatments (Fig. 5B). Carotenoids levels were similar in control, DS and UV-B plants, but decreased in DS + UV-B plants (Fig. 5C).

Electrolyte leakage in UV-B plants was higher than in control plants (Fig. 6A). The levels of MDA were highest in the DS plants (Fig. 6B). The antiradical activity ($ABTS^{+\bullet}$) increased in DS, UV-B and DS + UV-B plants (Fig. 6C). The levels of total phenols in DS and DS + UV-B plants were also higher than in the control and UV-B plants (Fig. 6D). Moreover, DS plants showed the highest levels of total phenols. Concerning catechols, plants exposed to the UV-B treatment showed the highest levels, followed by the DS + UV-B plants. The lowest levels of catechols were observed in control and DS plants (Fig. 6E). Flavonoids levels were higher in UV-B and DS + UV-B plants, followed by DS plants (Fig. 6F).

Discussion

A. pavonina leaves are a source of important nutraceutical compounds, and their composition is characterized here. *A. pavonina* leaves are rich in fatty acids, particularly the

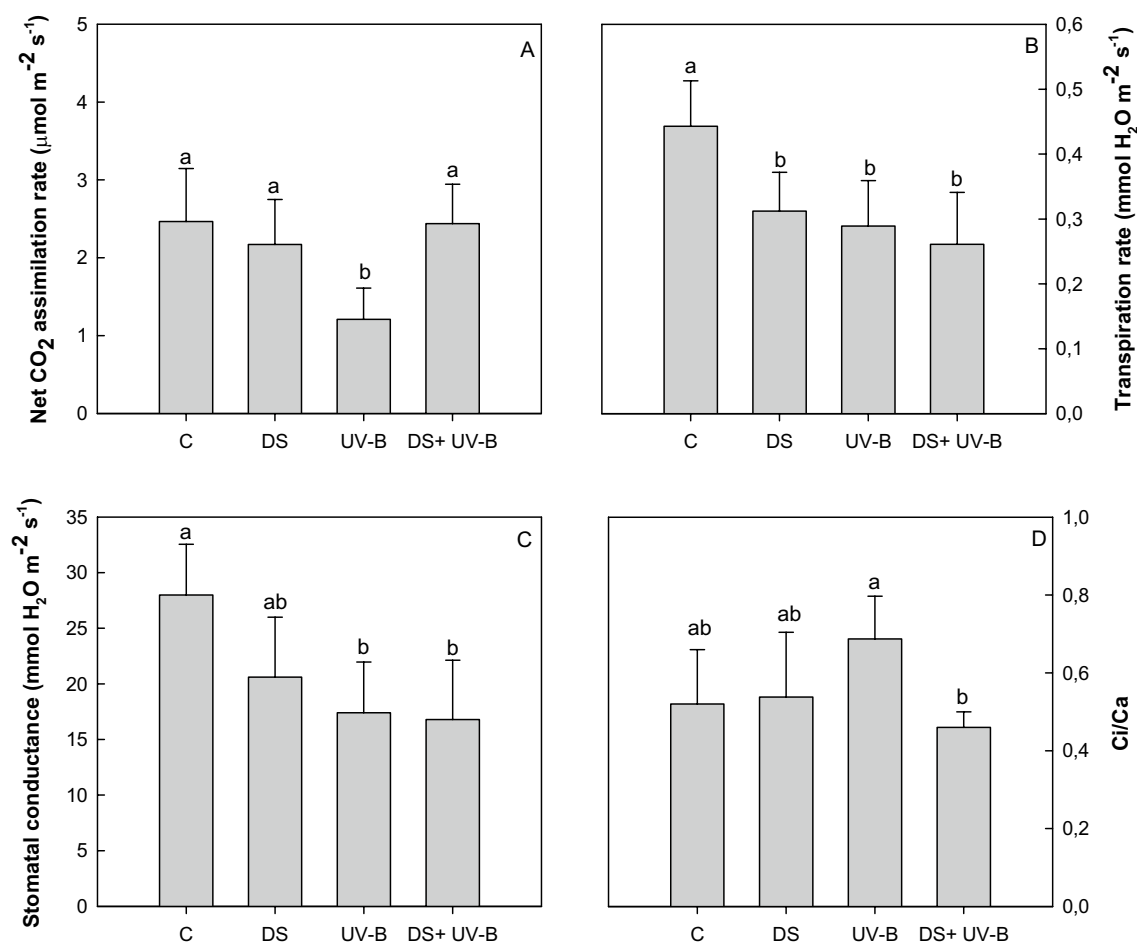


Fig. 4 Net CO₂ assimilation rate, transpiration rate, stomatal conductance and ratio of intercellular CO₂ and extracellular CO₂ concentration (Ci/Ca) in control, DS, UV-B and DS+UV-B plants of

A. pavinina. Values are means ± standard deviation ($n=5$ for C and $n=8$ for DS, UV-B, and DS+UV-B). Different letters mean statistical differences between treatments ($p < 0.05$)

polyunsaturated α -linolenic and linoleic acids that are associated with reduced risk of cardiovascular disease (Sokoła-Wysocka et al. 2018), antioxidants and carbohydrates, and metabolites related with TCA cycle, which act in controlling multiple diseases (Martínez-Reyes and Chandel 2020). In addition, a long-chain fatty alcohol, the triacnolol, with anticancer characteristics (Zhou et al. 2018) was identified in high amounts, highlighting this species' the industrial potential.

Our work also demonstrates that climate change-related episodes of drought and/or high UV-B irradiance can affect leaves' metabolism to enable plants to counteract these stress conditions' negative effects. These metabolic adaptations enriched its antioxidant potential and fatty acids pool, increasing the leaves' nutritional quality. Previous GC-MS analyses of *A. pavinina* leaf extracts also showed high amounts of triterpene squalene (a compound with ROS scavenger properties), and the anticancer compound phytol (Geronço et al. 2020).

DS and DS+UV-B activated some stress protection mechanisms related to water loss, like reducing stomata conductance and transpiration rate, which, however, did not prevent the plant from reducing its RWC. Both treatments induced a loss of the plant water status, but being the RWC values above 80%, the plants were subjected to moderate water deficit (Dias et al. 2014). This relation between H₂O movement and stomata aperture was particularly strong in the DS and DS+UV-B plants, as suggested by the positive correlation between RWC and transpiration rate ($r > 0.74$ and $p < 0.02$). Stomata closure is considered one of the first responses of plants to water deficit. Besides water deficit, stomata movements are also influenced by other factors such as UV-B radiation. It has been reported that the fluence and dose of UV-B can induce closure or opening of the stomata (Jansen 2002). Our data corroborate these findings, showing that the excessive UV-B promoted stomata closure. Besides restricting water movement, stomata closure also controls CO₂ influx, reducing net CO₂ assimilation rate (Dias et al.

Table 1 Lipophilic profile in C, DS, UV-B and DS + UV-B plants of *A. pavonina*

Rt (min)	Compound	Treatments				Fold Change		
		C (ng mg ⁻¹ DW)	DS (ng mg ⁻¹ DW)	UV-B (ng mg ⁻¹ DW)	DS+UV-B (ng mg ⁻¹ DW)	-3.8	0	+3.7
Alcohols								
67.1	Triacantanol	38.8±2.28a	17.1±2.09b	42.4±5.02a	Nd			
39.1	Myo-inositol	6.95±0.43a	1.06±0.07c	3.95±0.19b	Nd			
16.4	Glycerol	9.28±1.37a	4.76±0.30b	8.18±0.68a	Nd			
Carboxylic acids								
42.8	Stearic acid	7.99±0.35d	73.7±0.48a	43.9±0.55b	35.0±0.77c			
42.2	α -Linolenic acid	27.2±2.14d	83.1±0.69a	59.6±0.82b	36.3±0.01c			
42.1	Linoleic acid	15.0±1.32d	76.2±0.42a	48.1±0.43b	34.8±0.10c			
38.4	Palmitic acid	18.2±0.42d	83.0±1.00a	53.3±1.12b	37.0±0.50c			
35.8	Coumaric acid	11.6±0.56c	71.9±0.41a	43.9±0.36b	Nd			
32.8	Citric acid	10.1±1.56c	71.8±0.32a	47.2±1.71b	Nd			
25.6	Threonic acid	5.17±1.33c	70.1±0.05a	39.5±0.66b	Nd			
23.5	Malic acid	50.1±8.38b	84.4±2.05a	80.0±2.28a	34.2±0.06c			
21.8	Undecanoic acid	7.29±0.71b	Nd	40.1±1.22a	Nd			
16.8	Butenoic acid	5.55±1.00b	Nd	39.3±0.46a	Nd			
16.0	Pipecolic acid	5.03±1.47c	Nd	39.3±0.48a	34.4±0.24b			
7.1	Oxalic acid	7.39±0.75c	90.5±4.87a	44.9±5.37b	36.6±1.29b			
Carbohydrates								
50.4	Sucrose	164±11.9a	78.9±4.85c	114±1.31b	Nd			
50.2	Turanose	7.60±0.90a	Nd	3.84±0.16b	4.83±0.15b			
49.0	D-Trehalose	7.68±0.95	Nd	Nd	Nd			
48.3	3- α -Mannobiose	5.21±0.59a	Nd	4.14±0.31b	Nd			
36.9	D-Glucose isomer I	46.5±2.54a	29.2±1.72c	38.9±0.78b	3.19±0.13d			
34.6	D-Glucose isomer II	31.4±1.40a	20.0±0.63c	26.8±0.85b	2.90±0.09d			
33.4	β -D-Galactofuranose	5.99±1.04ab	7.01±0.80a	4.83±0.20b	Nd			
32.5	Fructose	4.52±0.19b	6.19±0.13a	4.45±0.21b	Nd			
32.3	D-(-)-Tagatofuranose	7.22±0.44a	7.30±0.56a	6.25±0.35a	Nd			

Values are means \pm standard deviation (n=4). For each line, different letters mean statistical differences between treatments ($p < 0.05$). Fold changes [Log_2 of (DS/C), UV-B/C) and (DS + UV-B/C)] of metabolites
Nd not detected

2014). In *A. pavonina* the UV-B treatment impaired net CO₂ assimilation rate and this reduction was more related with biochemical limitation, as suggested by the increase of Ci/Ca ($r = -0.77$ and $p = 0.002$). The photosynthetic apparatus is one of the main action targets of the UV-B radiation (Kataria et al. 2014). However, the effects of UV-B radiation on photosynthesis depend on several conditions, such as UV-B dose, flow rate and also PAR/UV-B radiation, plant growth stage and the interaction with other stresses (Kataria et al. 2014). For instance, UV-B conditions can increase oxidative stress and reduce photosynthesis (decrease of chlorophyll levels, reduction of RuBisCO enzyme activity and content, degradation of D1 and D2 proteins in PSII) (Reyes et al. 2019). Consequently, low photosynthetic carbon fixation led to unbalances between carbon assimilation and storage, resulting in reduced plant biomass production and ultimately in lower growth and productivity (Stitt et al. 2010; Reyes et al. 2019).

A different pattern of the response of *A. pavonina* plants was observed in the light-dependent reactions of photosynthesis. For the UV-B treatment, Φ_{PSII} was not affected and did not influence the net CO₂ assimilation rate ($r = 0.38$ and $p = 0.20$). This leads us to assume that possible biochemical restrictions (e.g., RuBisCO activity and content decrease) could be the main cause of net CO₂ assimilation reduction

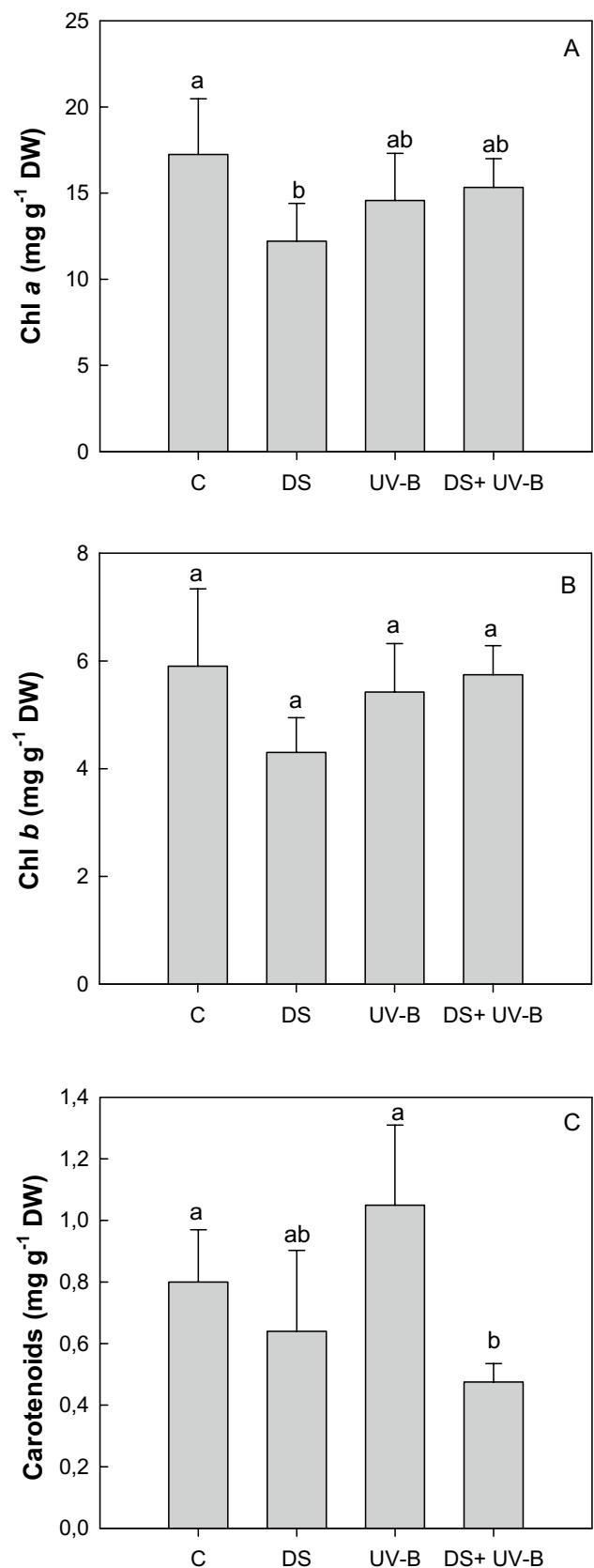
in UV-B plants, as suggested for other species exposed to UV-B (Fedina et al. 2010; Dias et al. 2018). However, the Φ_{PSII} values in DS and DS + UV-B plants were affected, but, as discussed above, did not strongly influence the net CO₂ assimilation rate in plants of this treatment. The causes for Φ_{PSII} reductions can be mainly associated with the decline in the Chl *a* content in DS plants ($r = 0.63$ and $p = 0.03$), instead of F_v/F_m ($r = 0.52$ and $p = 0.06$) and F_v'/F_m' reduction ($r = 0.48$ and $p = 0.06$). In turn, in the DS + UV-B plants, the F_v/F_m reduction contributed more to the Φ_{PSII} loss ($r = 0.60$ and $p = 0.04$).

Carbohydrates are key end products of photosynthesis and play a critical role as energy resources. In *A. pavonina*, despite the net CO₂ assimilation rate having the highest decrease in UV-B plants, a trend of reduced carbohydrates levels was notorious in plants of all stress treatments. This decline of leaf carbohydrate richness also might represent an increase in carbohydrates' catabolism (e.g., for cellular maintenance), or shifts in metabolic pathways (e.g., favouring the synthesis of compounds with a more important role in stress protection and adaptation) (Fig. 7). For instance, the TCA cycle metabolites oxalic, malic, citric, pipecolic and threonic acids, which play central roles in stress response (Návarová et al. 2012; Hu et al. 2015; Xu et al. 2016; Marček et al. 2019), accumulated in *A. pavonina* stressed plants

Fig. 5 Chlorophyll *a* and *b*, and carotenoids contents in control, DS, UV-B and DS+UV-B plants of *A. pavonina*. Values are means \pm standard deviation ($n=6$). Different letters mean statistical differences between treatments ($p < 0.05$)

(Fig. 7) and are negatively correlated with some main carbohydrates (correlation between oxalic, pipecolic, malic, citric and threonic acids with sucrose and glucose isomer I: $r \geq -0.90$ and $p \leq 0.003$; and between oxalic, pipecolic, malic and citric with glucose isomer II: $r \geq -0.90$ and $p \leq 0.002$), supporting the metabolic shift hypothesis, specifically in DS and DS+UV-B plants. Higher levels of TCA intermediates (e.g., citric and malic acids) were found in stressed *Cynodon transvaalensis* \times *C. dactylon*, *Poa pratensis*, and *Festuca arundinacea* plants, which reflected a higher mitochondrial activity for energy production (Hu et al. 2015). Also, the accumulation of oxalic and malic acids, and the non-protein amino acid pipecolic, is described to be related to osmoregulation and/or antioxidant processes under drought conditions (You et al. 2019), while threonic acid accumulation was also reported in response to oxidative stress (Navascués et al. 2012). These accumulations imply changes in primary and secondary metabolisms, as for example, oxalic acid results from carbohydrate metabolism and photosynthesis oxidative processes (Gouveia et al. 2020), and threonic acid is the main product from ascorbic acid metabolism (Navascués et al. 2012).

Besides TCA cycle metabolites, the accumulation of the fatty acids stearic, linolenic, linoleic, and palmitic was promoted by the stress conditions (Fig. 7). Moreover, these fatty acids' accumulation shows a consistent negative correlation with some sugars in most conditions. For example, the negative correlation between these fatty acids with sucrose and glucose ($r \geq -0.97$ and $p \leq 0.001$) in DS plants, with sucrose, glucose, turanose, 3- α -mannobiose and D-(-)-tagatofuranose ($r \geq -0.85$ and $p \leq 0.007$) in UV-B plants, and with glucose and turanose ($r \geq -0.94$ and $p \leq 0.001$) in DS+UV-B plants, highlights the putative metabolic shift of carbohydrates pathways to fatty acids production. Fatty acids increase may represent a source of energy reserve available to overcome the stress condition better. Considering that fatty acids are the main components of biomembranes and one of the main targets of the ROS (Liu et al. 2019), it is interesting to notice that *A. pavonina* responds to stress treatments by reducing the membrane fluidity (decrease of the ratio of unsaturated to saturated fatty acid, C = 1.6; DS = 1.0; UV-B = 1.1; and DS+UV-B = 0.9). Still, some oxidative damages occurred (UV-B-induced lipid peroxidation, and DS increased CMP). This suggests that *A. pavonina* may adapt to the stresses by adjusting its membrane fatty acid quantities that help stabilize the membrane fluidity and alleviate the stress damage (Liu et al. 2019). Besides this stress protective mechanism, *A. pavonina* also increased the levels of other antioxidants.



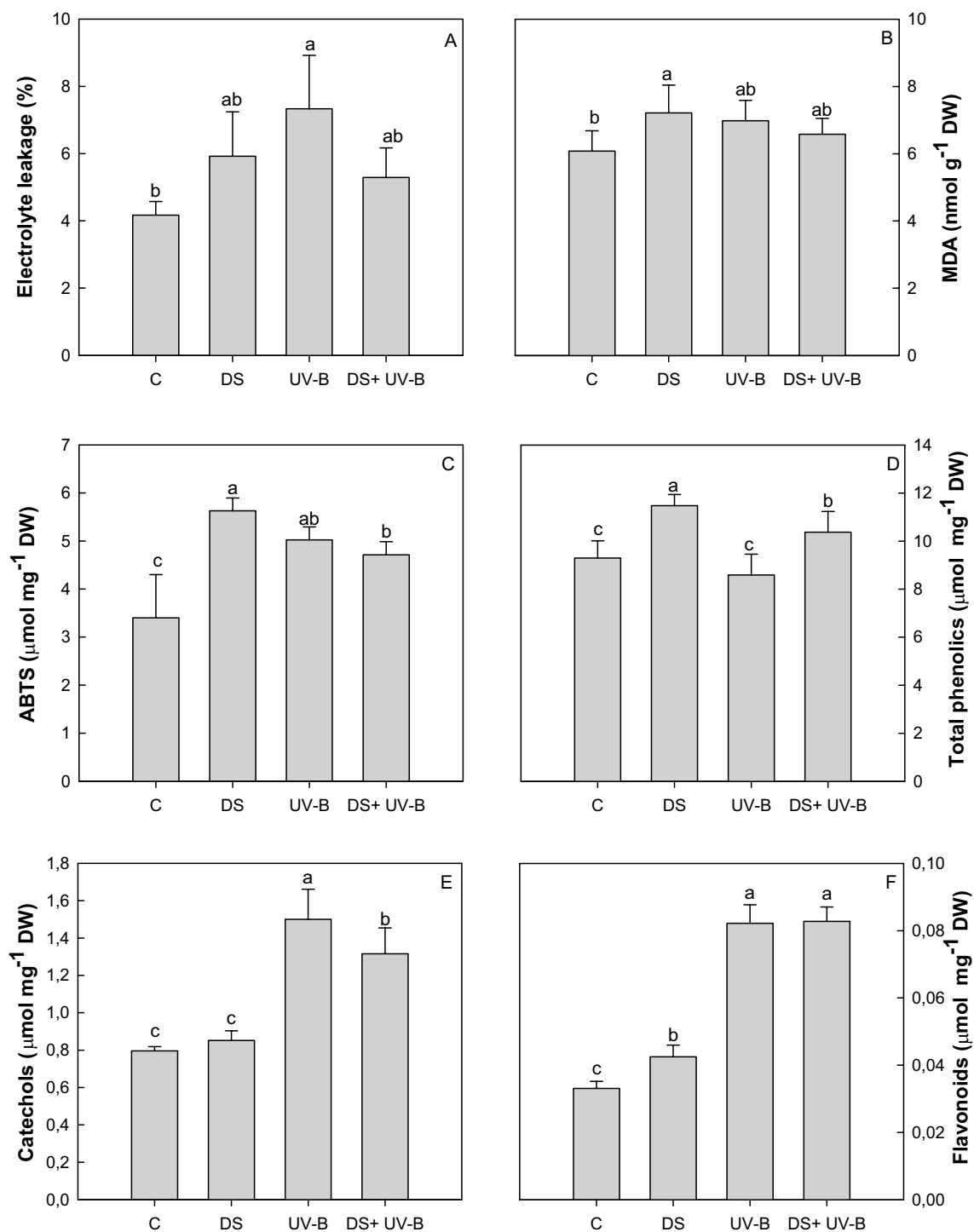


Fig. 6 Electrolyte leakage, MDA, ABTS, total polyphenol, catechols and flavonoids in control, DS, UV-B and DS+UV-B plants of *A. pavonina*. Values are means \pm standard deviation ($n=7$ for flavonoids

and catechols, and $n=8$ for electrolyte leakage, MDA, ABTS and total phenols). Different letters mean statistical differences between treatments ($p < 0.05$)

For instance, DS stressed plants preferably used coumaric acid, total phenolics, flavonoids, and catechols to control lipid peroxidation and/or membrane leakage ($r > 0.58$ and $p \leq 0.03$), while in UV-B or DS+UV-B plants the catechols

and flavonoids ($r > 0.61$ and $P \leq 0.03$) were more solicited. These antioxidants are potent reactive oxygen species (ROS) scavengers and also may act as UV-B filters (Agati et al. 2012). These data evidence that the levels and type

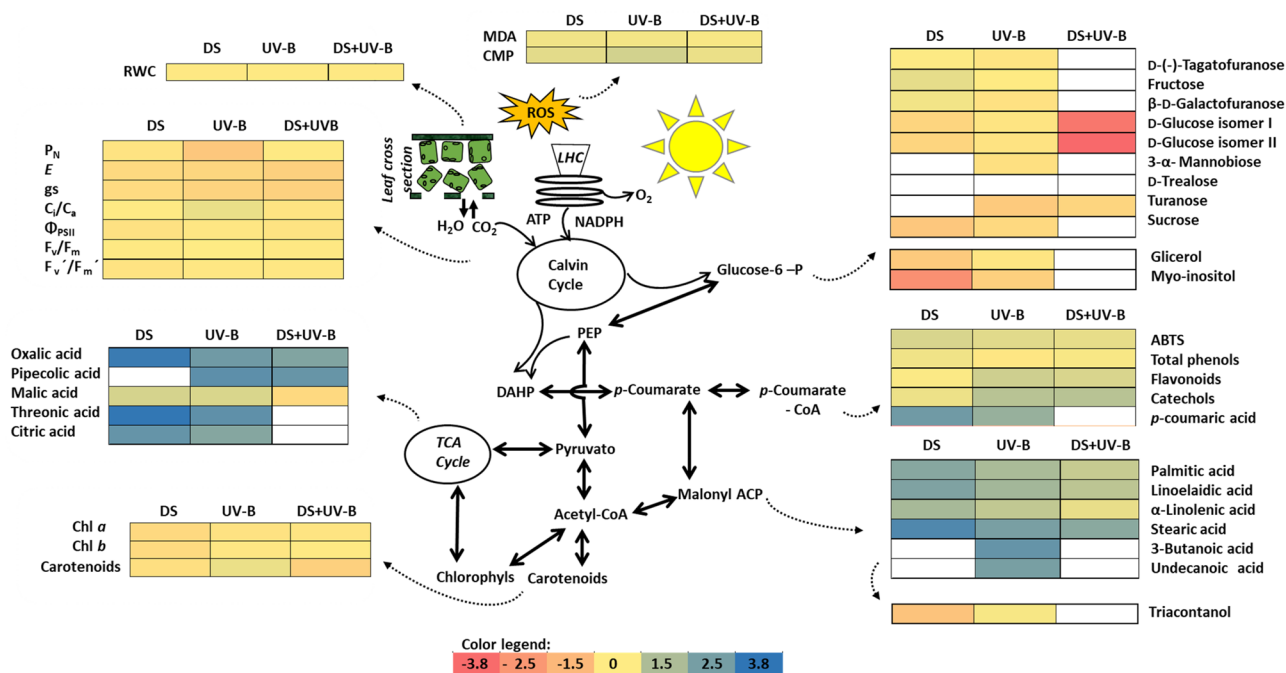


Fig. 7 General overview of the metabolites change in *A. pavanina* leaves after DS, UV-B and combined DS + UV-B treatments. Relative levels [expressed as \log_2 (DS/control or UVB/control or DS + UV-B/control)] are given besides each identified metabolite as a heatmap.

White rectangles means metabolites not identified in the respective treatment. P_N – net CO_2 assimilation rate; E – transpiration rate; g_s – stomatal conductance

of antioxidants in *A. pavanina* leaves can be modulated by DS, UV-B, and DS + UV-B conditions, contributing to the economical valorisation of this medicinal species.

The medium-chain fatty acid, undecanoic acid, can be found in small levels in several plant species (Doležalová et al. 2010). Undecanoic acid has antimicrobial and antibiofilm properties against various human pathogens and can be used in plant pest management (insects and nematodes) (Cruz-Estrada et al. 2018). The acid's specific role in plant response to abiotic stress is not clear, but its increase under high UV-B conditions suggests a protective role against this type of radiation. Another fatty acid that responds only to UV-B treatment is butanoic acid. Its accumulation in *A. pavanina* plants exposed to UV-B highlights its putative involvement in its stress acclimation (Hu et al. 2015). Interestingly, these two fatty acids' protective role was not evident when UV-B was combined with water deficit (Fig. 7), which deserves further studies.

The long-chain fatty alcohol, triacontanol, is a plant growth stimulant that promotes chlorophyll synthesis, photosynthesis, and growth, but also down-regulates stress factors (alleviating stress negative effects) (Naeem et al. 2011). *A. pavanina* leaves from control and UV-B plants are rich in this compound, but the DS and DS + UV-B conditions reduced triacontanol accumulation (Fig. 7). The particular role of this compound in DS (and DS + UV-B) response is not clear and deserves further

investigation, but could be related to specific oxidative stress and antioxidant response specifically mediated by drought (triacontanol vs MDA: $r = -0.836$, and $p = 0.001$; triacontanol vs total phenols and catechols $r > -0.82$ and $p < 0.004$).

Other compounds, like polyols such as myo-inositol and glycerol were also identified in *A. pavanina* leaves and were negatively controlled by DS and UV-B conditions (Fig. 7). Besides their important role as carbon and energy sources, and as osmolytes, polyols may also act as stress signalling molecules, thereby modulating the plants' response to stresses (Bhattacharya and Kundu 2020). Down and up-regulation of myo-inositol and glycerol levels by UV-B conditions and DS were reported in several species (Conde et al. 2015; Lytvyn et al. 2016), which may represent induction of protective mechanisms against abiotic stresses (Lytvyn et al. 2016). For instance, in *A. pavanina* these polyols are negatively correlated with some antioxidants (UV-B: myo-inositol vs flavonoids and catechols $r \geq -0.94$ and $p \leq 0.001$; and DS: myo-inositol and glycerol vs TAA, total phenols, flavonoids and catechols $r \geq -0.79$ and $p \leq 0.04$).

Conclusions

We have characterized the antioxidant and GC–MS profile of the industrially emerging medicinal species *A. pavanina*, demonstrating that their leaves are a source of important fatty acids, fatty alcohols, TCA cycle-related metabolites antioxidants, and carbohydrates. Moreover, we showed for the first time that this species copes with DS, UV-B, and DS + UV-B stress by adjusting its physiological performance and activating several stress protective mechanisms that eventually increase the nutritional and bioactive richness quality of these leaves, and thus its commercial value. Despite being associated with climate changes, UV-B, DS, or their combination can induce eustress in industrial plantations towards controlling and manipulating the nutritional and antioxidant richness of *A. pavanina* leaves, contributing, in this way, to the valorisation of this medicinal species and strengthening its potential for industrial exploitation.

Author contribution statement MC Dias and C Santos planned and coordinated the experiment; M Costa and MC Dias performed the physiological analysis; MC Dias, D Pinto, and AMS Silva performed the metabolomic analysis; MC Dias wrote the manuscript with contributions of all authors.

Supplementary Information The online version contains supplementary material available at <https://doi.org/10.1007/s11738-023-03622-8>.

Acknowledgements This work was financed by Fundação para a Ciência e Tecnologia (FCT) and Ministério da Educação e Ciência through national funds and the co-funding by the FEDER, within the PT2020 Partnership Agreement, and COMPETE 2010, within the projects CEF UI0183 – UID/BIA/04004/2020 and LAQV-REQUIMTE UIDB/50006/2020. MCDias (SFRH/BPD/100865/2014) was funded by national funds (OE), through FCT, I.P., in the scope of the framework contract foreseen in the numbers 4-6 of the article-23, of the Decree-Law 57/2016, August 29, changed by Law 57/2017, July 19.

Funding Open access funding provided by FCT/IFCCN (b-on). Fundação para a Ciência e Tecnologia, SFRH/BPD/100865/2014, Maria Celeste Pereira Dias.

Data availability Data available on request from the authors.

Declarations

Conflict of interest The authors declare that they have no conflict of interest.

Open Access This article is licensed under a Creative Commons Attribution 4.0 International License, which permits use, sharing, adaptation, distribution and reproduction in any medium or format, as long as you give appropriate credit to the original author(s) and the source, provide a link to the Creative Commons licence, and indicate if changes were made. The images or other third party material in this article are included in the article's Creative Commons licence, unless indicated

otherwise in a credit line to the material. If material is not included in the article's Creative Commons licence and your intended use is not permitted by statutory regulation or exceeds the permitted use, you will need to obtain permission directly from the copyright holder. To view a copy of this licence, visit <http://creativecommons.org/licenses/by/4.0/>.

References

- Acevedo-Rodríguez P, Strong MT (2012) Catalogue of the seed plants of the west Indies. Smithsonian Institution, Washington, p 1192
- Agati G, Azzarello E, Pollastri S, Tattini M (2012) Flavonoids as antioxidants in plants: location and functional significance. *Plant Sci* 196:67–76. <https://doi.org/10.1016/j.plantsci.2012.07.014>
- Araújo M, Santos C, Costa M, Moutinho-Pereira J, Correia C, Dias MC (2016) Plasticity of young *Moringa oleifera* L. plants to face water deficit and UVB radiation challenges. *J Photo Photobiol* b: Biol 162:278–285. <https://doi.org/10.1016/j.jphotobiol.2016.06.048>
- Bhattacharya S, Kundu A (2020) Sugars and sugar polyols in over-coming environmental stresses. In: Roychoudhury A, Tripathi DK (eds) Protective chemical agents in the amelioration of plant abiotic stress: biochemical and molecular perspectives. Wiley Online Library
- Brito C, Gonçalves A, Silva E, Martins S, Pinto L, Rocha L, Arrobas M, Rodrigues AA, Moutino-Pereira J, Correia C (2021) Kaolin foliar spray improves olive tree performance and yield under sustained deficit irrigation. *Sci Hort* 277:109795–109795. <https://doi.org/10.1016/j.scienta.2020.109795>
- Brunetti C, Ferdinando DM, Fini A, Pollastri S, Tattini M (2013) Flavonoids as antioxidants and developmental regulators: relative significance in plants and humans. *Int J Mol Sci* 14:3540–3555. <https://doi.org/10.3390/ijms14023540>
- Conde A, Regalado A, Rodrigues D, Costa M, Blumwald E, Chaves MM, Gerós H (2015) Polyols in grape berry: transport and metabolic adjustments as a physiological strategy for water-deficit stress tolerance in grapevine. *J Exp Bot* 66:889–906. <https://doi.org/10.1093/jxb/eru446>
- Correia CM, Coutinho JF, Bacelar EA, Gonçalves BM, Björn LO, Moutinho-Pereira J (2012) Ultraviolet-B radiation and nitrogen affect nutrient concentrations and the amount of nutrients acquired by above-ground organs of maize. *The Sci World J* 608954:1–11. <https://doi.org/10.1100/2012/608954>
- Cruz-Estrada A, Ruiz-Sánchez E, Cristóbal-Alejo J, González-Coloma A, Andrés MF, Gamboa-Angulo M (2018) Medium-chain fatty acids from *Eugenia winzerlingii* leaves causing insect settling deterrent, nematicidal, and phytotoxic effects. *Front Micro* 24:1724. <https://doi.org/10.3389/fmicb.2018.02835>
- Dias MC, Azevedo C, Costa M, Pinto G, Santos C (2014) *Melia azedarach* plants show tolerance properties to water shortage treatment: an ecophysiological study. *Plant Physiol Biochem* 75:123–127. <https://doi.org/10.1016/j.plaphy.2013.12.014>
- Dias MC, Figueiredo C, Pinto DCGA, Freitas H, Silva AMS, Santos C (2018) Heat shock and UV-B episodes modulate olive leaves lipophilic and phenolic metabolite profiles. *Ind Crop Prod* 133:269–275. <https://doi.org/10.1016/j.indcrop.2019.03.036>
- Dias MC, Pinto DCGA, Freitas H, Santos C, Silva AMS (2020a) The antioxidant system in *Olea europaea* to enhanced UV-B radiation also depends on flavonoids and secoiridoids. *Phytochemistry* 170:112199. <https://doi.org/10.1016/j.phytochem.2019.112199>
- Dias MC, Santos C, Silva S, Pinto DCGA, Silva AMS (2020b) Physiological and metabolite reconfiguration of *Olea europaea* to cope

- and recover from a heat or high UV-B shock. *J Agri Food Chem* 68:11339–11349. <https://doi.org/10.1021/acs.jafc.0c04719>
- Doležalová M, Janiš R, Svobodová H, Kašpárková V, Humpolíček P, Krejčí J (2010) Antimicrobial properties of 1-monoacylglycerols prepared from undecanoic (C11:0) and undecenoic (C11:1) acid. *Eur J Lip Sci Tec* 112:1106–1114. <https://doi.org/10.1002/ejlt.200900295>
- Escobar-Bravo R, Nederpel C, Naranjo S, Kim HK, Rodríguez-López MJ, Chen G, Glauser G, Leiss KA, Klinkhamer PGL (2021) Ultraviolet radiation modulates both constitutive and inducible plant defenses against thrips but is dose and plant genotype dependent. *J Pest Sci* 94:69–81. <https://doi.org/10.1007/s10340-019-01166-w>
- Fedina I, Hidema J, Velitchkova V, Georgieva K, Nedeva D (2010) UV-B induced stress responses in three rice cultivars. *Biol Plant* 54:571–574. <https://doi.org/10.1007/s10535-010-0102-3>
- Geronço MS, Melo RC, Barros HLM, Aquino SR, Oliveira FCE, Islam MT, Pessoa C, Rizzo MS, Costa MP (2020) Advances in the research of *Adenantha pavonina*: from traditional use to intellectual property. *J Med Plant Res* 14:24–53. <https://doi.org/10.5897/JMPR2019.6872>
- Giertych MJ, Karolewski P, de Temmerman LO (1999) Foliage age and pollution alter content of phenolic compounds and chemical elements in *Pinus nigra* needles. *Water Air Soil Pol* 110:363–377. <https://doi.org/10.1023/A:1005009214988>
- Gouveia CSS, Ganança JFT, Lebot V, Carvalho MAAP (2020) Changes in oxalate composition and other nutritive traits in root tubers and shoots of sweet potato (*Ipomoea batatas* L. [Lam.]) under water stress. *J Sci Food Agri* 100:1702–1710. <https://doi.org/10.1002/jsfa.10185>
- Gupta A, Singh PP, Singh P, Singh K, Singh AV, Singh KS, Kumar A (2019) Medicinal plants under climate change: impacts on pharmaceutical properties of plants. Climate change and agricultural ecosystems current. Elsevier
- Hodges DM, DeLong JM, Forney CF, Prange RK (1999) Improving the thiobarbituric acid-reactive-substances assay for estimating lipid peroxidation in plant tissues containing anthocyanin and other interfering compounds. *Planta* 207:604–611. <https://doi.org/10.1007/s004250050524>
- Hu T, Liu S-Q, Amombo E, Fu J-M (2015) Stress memory induced rearrangements of HSP transcription, photosystem II photochemistry and metabolism of tall fescue (*Festuca arundinacea* Schreb.) in response to high-temperature stress. *Front Plant Sci* 6:403. <https://doi.org/10.3389/fpls.2015.00403>
- Huang H, Ullah F, Zhou D-X, Yi M, Zhao Y (2019) Mechanisms of ROS regulation of plant development and stress responses. *Front Plant Sci* 10:800. <https://doi.org/10.3389/fpls.2019.00800>
- IPCC - Impacts, adaptation, and vulnerability (2014) Part A Global and sectoral aspects. In: Field CB (ed) Contribution of working group II to the fifth assessment report of the intergovernmental panel on climate change. Cambridge University Press, Cambridge
- Jansen MAK (2002) Ultraviolet-B radiation effects on plants: induction of morphogenic responses. *Physiol Plant* 116:423–429. <https://doi.org/10.1034/j.1399-3054.2002.1160319.x>
- Kataria S, Jajoo A, Guruprasad KN (2014) Impact of increasing ultraviolet-B (UV-B) radiation on photosynthetic processes. *J Photochem Photobiol B Biol* 137:55–66. <https://doi.org/10.1016/j.jphotobiol.2014.02.004>
- Liu X, Ma D, Zhang Z, Wang S, Du S, Deng X, Yin L (2019) Plant lipid remodelling in response to abiotic stresses. *Env Exp Bot* 165:174–184. <https://doi.org/10.1016/j.envexpbot.2019.06.005>
- López-Orenes A, Dias MC, Ferrer MA, Calderón A, Moutinho-Pereira J, Correia C, Santos C (2018) Different mechanisms of the metaliferous *Zygophyllum fabago* shoots and roots to cope with Pb toxicity. *Environ Sci and Poll Res* 25:1319–1330. <https://doi.org/10.1007/s11356-017-0505-1>
- Lytvyn DI, Raynaud C, Yemets AI, Bergounioux C, Blume B (2016) Involvement of inositol biosynthesis and nitric oxide in the mediation of UV-B induced oxidative stress. *Front Plant Sci* 7:430. <https://doi.org/10.3389/fpls.2016.00430>
- Ma Y, Dias MC, Freitas H (2020) Drought and salinity stress responses and microbe-induced tolerance in plants. *Front Plant Sci* 11:591911. <https://doi.org/10.3389/fpls.2020.591911>
- Machado F, Dias MC, Pinho PGD, Araújo AM, Pinto D, Silva A, Correia C, Moutinho-Pereira J, Santos C (2017) Photosynthetic performance and volatile organic compounds profile in *Eucalyptus globulus* after UVB radiation. *Environ Exp Bot* 140:141–149. <https://doi.org/10.1016/j.envexpbot.2017.05.008>
- Marček T, Hamow KA, Véghe B, Janda T, Darko E (2019) Metabolic response to drought in six winter wheat genotypes. *PlosOne* 14:e02124111. <https://doi.org/10.1371/journal.pone.0212411>
- Martínez-Reyes I, Chandel NS (2020) Mitochondrial TCA cycle metabolites control physiology and disease. *Nat Commun* 11:102. <https://doi.org/10.1038/s41467-019-13668-3>
- Naeem M, Khan MMA, Moinuddin (2011) Triacantanol: a potent plant growth regulator. *J Med Plant Int* 7:129–142. <https://doi.org/10.1080/17429145.2011.619281>
- Návarová H, Bernsdorff F, Döring AC, Zeier F (2012) Pipecolic acid, an endogenous mediator of defense amplification and priming, is a critical regulator of inducible plant immunity. *Plant Cell* 24:5123–5141. <https://doi.org/10.1105/tpc.112.103564>
- Navascués J, Pérez-Rontomé C, Sánchez DH, Staudinger C, Wienkoop S, Rellán-Álvarez R, Becana M (2012) Oxidative stress is a consequence, not a cause, of aluminum toxicity in the forage legume *Lotus corniculatus*. *New Phyt* 193:625–636. <https://doi.org/10.1111/j.1469-8137.2011.03978.x>
- Omidí H, Shams H, Sahandi M, Rajabian T (2018) Balangu (*Lallemantia* sp.) growth and physiology under field drought conditions affecting plant medicinal content. *Plant Physiol Bioch* 130:641–646. <https://doi.org/10.1016/j.plaphy.2018.08.014>
- Pearson K (1895) Notes on regression and inheritance in the case of two parents. *P R Soc London* 58:240–242
- PROSEA, Plant resources of Southeast Asia 2012 <https://www.nhbs.com/3/series/prosea-plant-resources-of-south-east-asia>
- Re R, Pellegrini N, Proteggente A, Pannala A, Yang M, Rice-Evans C (1999) Antioxidant activity applying an improved ABTS radical cation decolorization assay. *Free Rad Biol Med* 26:1231–1237. [https://doi.org/10.1016/S0891-5849\(98\)00315-3](https://doi.org/10.1016/S0891-5849(98)00315-3)
- Reyes H, Scartazza T, Pompeiano A, Guglielminetti L (2019) Physiological responses of *Lepidium meyenii* plants to ultraviolet-B radiation challenge. *BMC Plant Biol* 19:186. <https://doi.org/10.1186/s12870-019-1755-5>
- Schreiner M, Mewis I, Neugart S, Zrenner R, Glaab J, Wiesner M, Janson MAK (2016) UV-B Elicitation of secondary plant metabolites. In: Kneissl M, Rass J (eds) III-Nitride ultraviolet emitters, Springer Series in Materials Science. Springer, pp 387–414
- Sims DA, Gamon JA (2002) Relationships between leaf pigment content and spectral reflectance across a wide range of species, leaf structures and developmental stages. *Rem Sens Environ* 81:337–354. [https://doi.org/10.1016/S0034-4257\(02\)00010-X](https://doi.org/10.1016/S0034-4257(02)00010-X)
- Sokoła-Wysoczańska E, Wysoczański T, Wagner J, Czyż K, Bodkowski R, Lochyński S, Patkowska-Sokoła B (2018) Polyunsaturated fatty acids and their potential therapeutic role in cardiovascular system disorders. *Nutrients* 10:1561. <https://doi.org/10.3390/nu10101561>
- Stitt M, Lunn J, Usadel B (2010) Arabidopsis and primary photosynthetic metabolism - more than the icing on the cake. *Plant J* 61:1067–1091. <https://doi.org/10.1111/j.1365-313X.2010.04142.x>
- Wu X, Zhang S, Li X, Zhang F, Fan Y, Liu Q, Wan X, Lin T (2021) Postharvest UV-B radiation increases enzyme activity, polysaccharide and secondary metabolites in honeysuckle (*Lonicera*

- japonica* Thunb.). *Ind Crops Prod* 171:113907. <https://doi.org/10.1016/j.indcrop.2021.113907>
- Xu Z, Jiang Y, Ji B, Zhou G (2016) Elevated-CO₂ response of stomata and its dependence on environmental factors. *Front Plant Sci* 657:1–15. <https://doi.org/10.3389/fpls.2016.00657>. (PMID: 27242858)
- You J, Zhang Y, Liu A, Wang X, Dossa K, Zhou R, Yu J, Zhang Y, Wang L, Zhang X (2019) Transcriptomic and metabolomic profiling of drought-tolerant and susceptible sesame genotypes in response to drought stress. *BMC Plant Biol* 19:267. <https://doi.org/10.1186/s12870-019-1880-1>
- Zarnowski R, Jaromin A, Certik M, Czabany T, Fontaine J, Jakubik T, Iqbal MCM, Grandmougin-Ferjani A, Kozubek A, Pietr J (2004) The oil of *Adenantha pavonina* L. seeds and its emulsions. *Zeitschrift Für Naturforschung C - J Biosci* 59:321–326. <https://doi.org/10.1515/znc-2004-5-605>
- Zhou Y, Li N, Qiu Z, Lu X, Fang X, Chen X, Ren WG, Ouyang P (2018) Superior anti-neoplastic activities of triacontanol-PEG conjugate: synthesis, characterization and biological evaluations. *Drug Del* 25:1546–1559

Publisher's Note Springer Nature remains neutral with regard to jurisdictional claims in published maps and institutional affiliations.